MICROPLANE MODEL FOR FRACTURE ANALYSIS OF CONCRETE STRUCTURES

Zdeněk P. Bažant and Byung H. Oh

Center for Concrete and Geomaterials

The Technological Institute

Northwestern University, Evanston, IL. 60201

ABSTRACT

Dynamic fracture analysis of concrete structures necessitates a triaxial stress-strain relation that describes gradual strain-softening with reduction of tensile stress to zero. A new model which does that and is applicable under general loading, including rotating principal stress directions, is proposed. It is based on accumulating stress relaxations due to microcracking from the planes of all orientation within the microstructure. Comparisons with tensile test data are given.

Introduction

Fracture analysis of certain brittle heterogeneous materials, such as concretes and many rocks, requires consideration of progressive microcracking in the fracture process zone as the fracture is being formed. This type of fracture may be efficiently modeled with the crack band approach, in which the material behavior in the fracture process zone is described by a strain-softening triaxial stress-strain relation, provided that the strain-softening behavior is associated with a zone of a certain characteristic width that is treated as a material property or is determined in advance by stability analysis. A suitable triaxial stress-strain relation of the total strain type (deformation theory type) has been recently formulated and has been shown to lead to satisfactory agreement with essentially all existing fracture test data available in the literature [1, 2]. This stress-strain relation is, however, limited to situations in which the direction of the maximum principal stress does not significantly rotate during the fracture formation. This is not so in certain important situations, especially various dynamic problems. Here, a longitudinal wave may produce only a partial tensile fracture (i.e., distributed microcracking) and the fracture may be completed subsequently when a shear wave arrives, causing a principal tensile stress in a different direction. For such situations of progressive fracturing, it is necessary to develop a triaxial strain-softening stress-strain relation which is path-dependent and is formulated incrementally. A model called microplane model is developed to fill this need. We propose here a model in which the constitutive properties are characterized by a relation between the stresses and strains acting within the microstructure on planes of various orientation, called the microplanes. This formulation involves no tensorial invariance restrictions. The restrictions can then be satisfied by a suitable combination of planes of various orientation. E.g., in the case of isotropy, each orientation must be equally frequent. Thus, one circumvents the difficulty of setting up a general nonlinear constitutive equation in terms of proper invariants.

The idea of defining the inelastic behavior independently on planes of different orientation within the material, and then in some way superimposing the inelastic effects from all planes, appeared in Taylor's work [3] on plasticity of polycrystalline metals. Batdorf and Budianski [4] formulated the slip theory of plasticity, in which the stresses acting on various planes of slip are obtained by resolving the macroscopic applied stress, and the plastic strains (slips) from all planes are then superimposed. The same superposition of inelastic strains was used in the so-called multilaminate models of Zienkiewicz et al. [5] and Pande et al [6, 7] and in many works on plasticity of polycrystals. While the previous works dealing with plasticity of polycrystals [3, 4, 8, 9, 10-14] or soils [15,16] the stresses on various microplanes were assumed to be equal to the resolved macroscopic stress, this new model uses a similar assumption for part of the total strains.

Fundamental Hypotheses

The resultants of the stresses acting on the microplanes over unit areas of the macroscopic continuum will be called the microstresses s_{ij}, and the strains of the macroscopic continuum accumulated from the deformations on the microplanes will be called the microstrains, e_{ij}. With regard to the interaction between the micro-and macro-levels, one may introduce the following basic hypotheses.

Hypotehsis I. - The tensor of macroscopic strain, ϵ_{ij}, is a sum of a purely elastic macrostrain ϵ^a_{ij} that is unaffected by cracking, and an inelastic macrostrain ϵ_{ij} which reflects the stress relaxation due to cracking, i.e.,

$$\epsilon_{ij} = \epsilon^{a}_{ij} + e_{ij} \qquad (1)$$

Here, latin lower case subscripts refer to cartesian coordinates x_i (i = 1,2,3).

Hypothesis II. - The normal microstrain e_n which governs the progressive development of cracking on a microplane of any orientation is equal to the resolved macroscopic strain tensor e_{ij} for the same plane, i.e.,

$$e_n = n_i n_j e_{ij} \qquad (2)$$

in which n_i = direction cosines of the unit normal $\vec{n}$ of the microplane and the repeated latin lower case subscripts indicate a summation over 1, 2, 3.

Hypothesis III. - The stress relaxation due to all microcracks normal to $\vec{n}$ is characterized by assuming that the microstress s_n on the microplane of any orientation is a function of the normal microstrain e_n on the same plane, i.e.,

$$s_{\vec{n}} = (2\pi/3)\, F(e_n) \qquad (3)$$

The factor $(2\pi/3)$ is introduced just for convenience, as it will later cancel out.

The last hypothesis is similar to that made for shear microstresses and microstrains in the slip theory of plasticity. Hypothesis II is however opposite. There are three reasons for hypothesis II.

1. Using resolved stresses rather than resolved strains on the microplanes would hardly allow describing strain-softening, since in this case there are two strains corresponding to a given stress but only one stress corresponding to a given strain.

2. The microstrains must be stable when the macrostrains are fixed. It has been experienced numerically that, in the case of strain-softening, the model becomes unstable if resolved stresses rather than strains are used.

3. The use of resolved strains rather than resolved stresses seems to reflect the microstructure of a brittle aggregate material more realistically. The use of resolved stresses is reasonable for polycrystalline metals in which local slips scatter widely while the stress is roughly uniformly distributed throughout the microstructure. By contrast, in a brittle aggregate material consisting of hard inclusions embedded in a weak matrix, the stresses are far from uniform, having sharp extremes at the locations where the surfaces of aggregate pieces are nearest. The deformation of the thin layer of matrix between two aggregate pieces, which yields the major contribution to inelastic strain, is determined chiefly by the relative displacements of the centroids of the two aggregate pieces, which roughly correspond to the macroscopic strain. The microplanes may be imagined to represent the thin layers of matrix and the bond planes between two adjacent aggregate pieces, since microcracking is chiefly concentrated there.

In Hypotehsis III, the relaxation of shear microstresses s_{nt} caused by the shear and normal microstrains e_{nt} and e_n is neglected. This assumption is probably quite good for very small crack openings, since it has been deduced from test data on shearing of cracks in concretes that no relative shear displacements on the rough interlocked cracks is possible before a certain finite crack opening is produced, and that the shear stiffness of the cracks decreases rather slowly as the crack gradually opens. One must admit, however, that Eq. 3 (Hypothesis III) is also justified by its simplicity. It would be much more complicated to assume a general relation between the normal and shear microstresses and microstrains on each plane.

Tangential Stiffness Matrix

The virtual work of stresses per unit volume may be written, according to Eq. 1, as $\delta W = \sigma_{ij}\, \delta\epsilon_{ij} = \sigma_{ij}\, \delta\epsilon^{a}_{ij} + \sigma_{ij}\, \delta e_{ij}$. Summing the virtual work due to $\delta\epsilon^{a}_{ij}$ and δe_{ij}, we further have $\delta W = \sigma^{a}_{ij}\, \delta\epsilon^{a}_{ij} + s_{ij}\, \delta e_{ij}$, in which s_{ij} is the macrostress tensor resulting from s_n on all planes, and σ^{a}_{ij} is the stress tensor corresponding to ϵ^{a}_{ij}. Since both expressions for δW must hold for any $\delta\epsilon^{a}_{ij}$ and any δe_{ij}, we must have $s_{ij} = \sigma^{a}_{ij} = \sigma_{ij}$.

Equilibrium conditions may be expressed by means of the principle of virtual work:

$$\delta W^{c} = \frac{4}{3}\pi\, \sigma_{ij}\, \delta e_{ij} = 2 \int_S s_n\, \delta e_n\, f(\vec{n})\, dS \qquad (4)$$

in which S represents the surface of a unit hemisphere, the factor $(4\pi/3)$ is due to integrating over the surface of a sphere of radius 1, and $dS = \sin\phi\, d\theta\, d\phi$ (Fig. 1b). Note that we do not need to integrate over the entire surface of the sphere, since the values of σ_n or e_n are equal at any two diametrically opposite points on the sphere. Function $f(\vec{n})$ defines the relative frequency of the planes of various orientations $\vec{n}$, contributing to inelastic stress relaxation.

Substituting Eqs. 2-3 into Eq. 4, we get $\sigma_{ij}\, \delta e_{ij} = \int_S F(e_n)\, n_i\, n_j\, \delta e_{ij}\, f(\vec{n})\, dS$, and because this must hold for any δe_{ij}, we must have

$$\sigma_{ij} = \int_0^{2\pi} \int_0^{\pi/2} F(e_n)\, n_i\, n_j\, f(\vec{n})\, \sin\phi\, d\phi\, d\theta \qquad (5)$$

Furthermore, according to Eq. 2, $dF(e_n) = F'(e_n) de_n = F'(e_n) n_k\, n_m\, de_{km}$, and thus differentiation of Eq. 5 finally yields

$$d\sigma_{ij} = D^{c}_{ijkm}\, de_{km} \qquad (6)$$

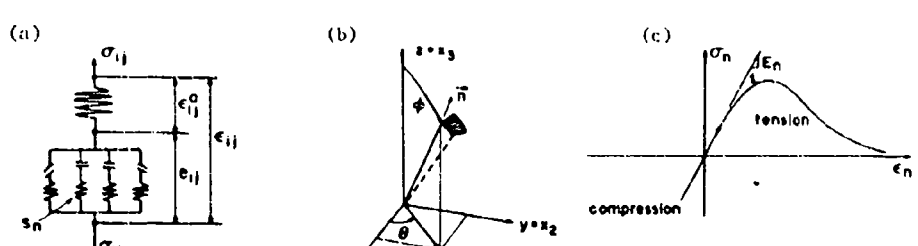

Fig. 1

Model of Strain Interaction, Spherical Coordinates, and Tensile Stress-Strain Diagram.

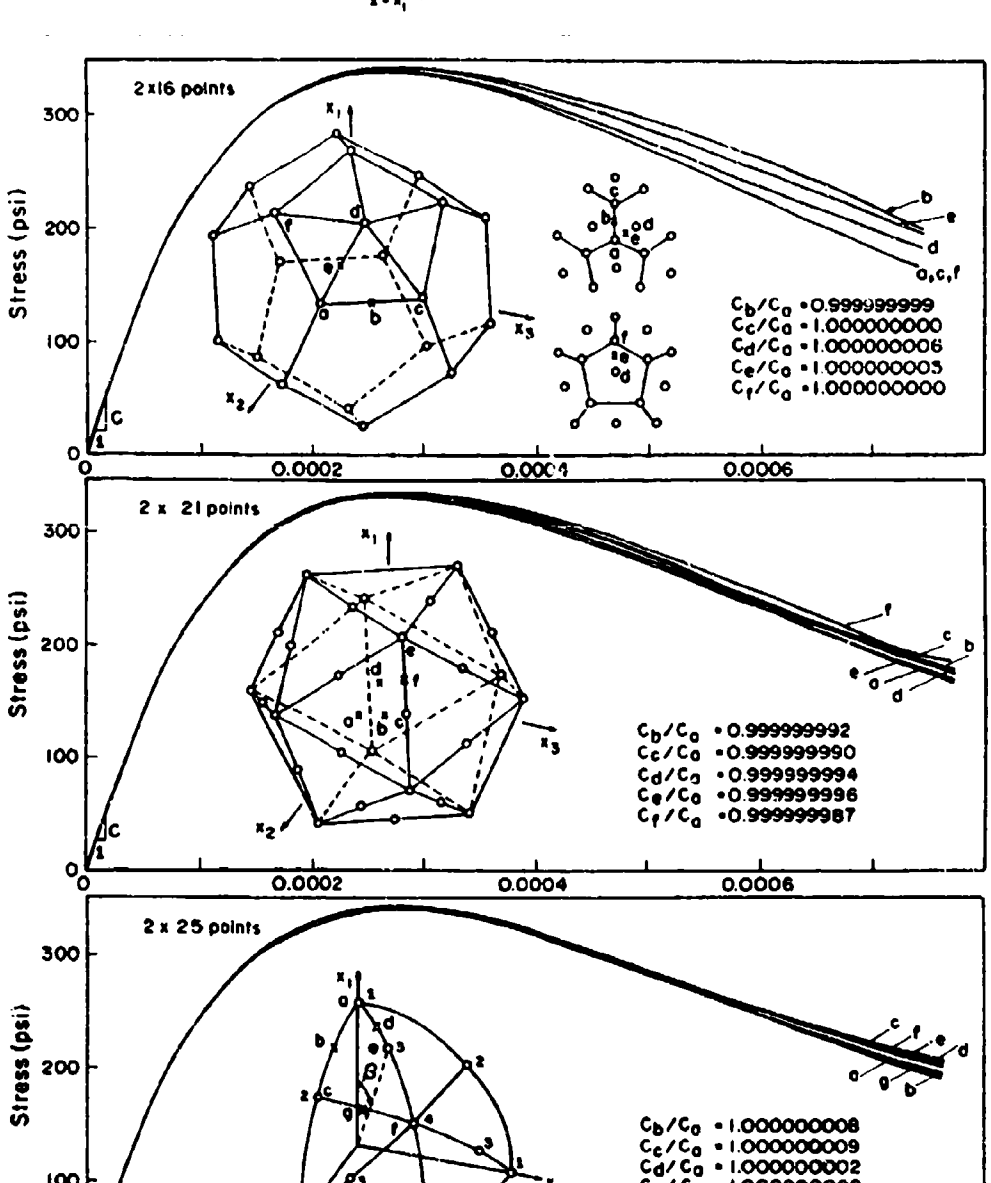

Fig. 2

Response Curves for Uniaxial Stress at Various Orientations

in which

$$D^c_{ijkm} = \int_0^{2\pi}\int_0^{\pi/2} a_{ijkm}\, F'(\epsilon_n)\, f(\vec{n})\, \sin\phi\, d\phi\, d\theta, \text{ with} \quad (7)$$

$$a_{ijkm} = n_i n_j n_k n_m$$

D^c_{ijkm} may be called the tangent stiffnesses of the microplane system. Note that the sequence of subscripts of D^c_{ijkm} is immaterial; therefore, there are only six independent values of incremental stiffnesses. Eq. 7 applies to initially anisotropic solids. For isotropic solids, we may substitute $f(\vec{n}) = 1$.

The mathematical structure of the present model may be geometrically visualized with the rheologic model in Fig. 1a.

The compliance corresponding to the additional elastic strain σ^a_{ij} must satisfy isotropy conditions, and so

$$C^a_{ijkm} = \frac{1}{9K^a}\,\delta_{ij}\,\delta_{km} + \frac{1}{2G^a}\left(\delta_{ik}\,\delta_{jm} - \frac{1}{3}\,\delta_{ij}\,\delta_{km}\right) \quad (8)$$

in which K^a and G^a are certain bulk and shear moduli which cannot be less than the actual initial bulk and shear moduli K and G. For fitting of test data, it was assumed, with success, that $1/G^a = 0$.

Recalling Eq. 1 (and Fig. 1a), we may now write the incremental stress-strain relation as

$$d\sigma_{ij} = D_{ijkm}\, d\epsilon_{ij}, \text{ with } [D_{ijkm}] = \left[(D^c)^{-1}_{ijkm} + (C^a_{ijkm})^{-1}\right] \quad (9)$$

Applying Eq. 7 to elastic deformations (with $f(\vec{n}) = 1$), one finds that the matrix in Eq. 7 always yields Poisson's ratio $\nu = 1/4$. This is because the slips on all microplanes are neglected. Since $\nu = 1/4$ is not quite true for concrete, the additional elastic strain must be used to make a correction. Let us now determine the value of K^a needed to achieve the desired Poisson's ratio ν. Let superscripts c and a distinguish between the values corresponding to D^c_{ijkm} and C^a_{ijkm}. For uniaxial stress we have $\epsilon_{11} = \sigma_{11}/9K^a + \sigma_{11}/E^c$ and $\epsilon_{22} = \sigma_{11}/9K^a - \nu^c\sigma_{11}/E^c$ in which $\nu^c = 1/4$ and $E^c = 2\pi E_n/5$, $E_n = F'(0)$ = initial normal stiffness for the microplane. Since $\epsilon_{22} = -\nu\epsilon_{11}$, we must have

$$K^a = \frac{1+\nu}{9(\nu^c - \nu)}\,E^c \qquad (\text{for } \nu \le \nu^c) \quad (10)$$

This is, of course, under the assumption that $1/G^a = 0$.

The stress-strain relation for the microplanes, relating σ_n to ϵ_n, must describe cracking all the way to complete fracture, at which σ_n reduces to zero. In view of the kinematics visualized in Fig. 1b, it is clear that σ_n as a function of ϵ_n must first rise, then reach a maximum, and then gradually decline to zero. We choose the final zero value to be attained asymptotically, since no precise information exists on the final strain at which $\sigma_n = 0$, and since a smooth curve is convenient computationally. The following expressions were used in computations [19] (Fig. 1c);

$$\text{for } \epsilon_n > 0: \quad \sigma_n = E_n\,\epsilon_n\, e^{-(k\epsilon_n^p)}, \qquad \text{for } \epsilon_n \le 0: \quad \sigma_n = E_n\,\epsilon_n \quad (11)$$

in which E_n, k, and p are positive constants; $k = 1.8 \times 10^7$, $p = 2$.

The integral in Eq. 7 has to be evaluated numerically, approximating it by a finite sum:

$$D^c_{ijkm} = \sum_{\alpha=1}^{N} w_\alpha [a_{ijkm}\, F'(\epsilon)]_\alpha \quad (12)$$

in which α refers to the values at certain numerical integration points on a unit hemisphere (i.e., certain directions), and w_α are the weights associated with the integration points.

Since in finite element programs for incremental loading the numerical integration needs to be carried out a great number of times, a very efficient numerical integration formula is needed. For the slip theory of plasticity, the integration was performed using a rectangular grid in the θ-ϕ plane. This formula is, however, computationally inefficient because the integration points are crowded near the poles, and also because in the θ-ϕ plane the singularity arising from the pole takes away the benefit from a use of higher-order integration formula.

Optimally, the integration points should be distributed over the spherical surface as uniformly as possible. A perfectly uniform subdivision is obtained when the microplanes normal to the α-directions are the sides of a regular polyhedron. A regular polyhedron with the most sides is the icosahedron, for which N = 10 (half the number of sides). Such a numerical integration formula was proposed by Albrecht and Collatz [18].

Numerical experience revealed, however, that 10 points are not enough when strain-softening takes place; it was found that the strain-softening curves calculated for uniaxial tensile stresses oriented at various angles with regard to the α-directions significantly differ from each other, even though within the strain-hardening range the differences are negligible. Therefore, more than 10 points are needed, and then a perfectly uniform

Table 1 - Direction Cosines and Weights for 2 x 21 Points (Orthogonal) $O(h^6)$

α	x_1^α	x_2^α	x_3^α	w^α
1	1	0	0	0.02652141274
2	0	1	0	"
3	0	0	1	"
4	0.7071067812	0.7071067812	0	0.01993014153
5	0.7071067812	-0.7071067812	0	"
6	0.7071067812	0	0.7071067812	"
7	0.7071067812	0	-0.7071067812	"
8	0	0.7071067812	0.7071067812	"
9	0	0.7071067812	-0.7071067812	"
10	0.3879072746	0.3879072746	0.8360956240	0.02507124272
11	0.3879072746	0.3879072746	-0.8360956240	"
12	0.3879072746	-0.3879072746	0.8360956240	"
13	0.3879072746	-0.3879072746	-0.8360956240	"
14	0.3879072746	0.8360956240	0.3879072746	"
15	0.3879072746	0.8360956240	-0.3879072746	"
16	0.3879072746	-0.8360956240	0.3879072746	"
17	0.3879072746	-0.8360956240	-0.3879072746	"
18	0.8360956240	0.3879072746	0.3879072746	"
19	0.8360956240	0.3879072746	-0.3879072746	"
20	0.8360956240	-0.3879072746	0.3879072746	"
21	0.8360956240	-0.3879072746	-0.3879072746	"

$\beta = 33.269905^\circ$

Table 2 - Direction Cosines and Weights for 2 x 25 Points. $O(h^{10})$.

α	x_1^α	x_2^α	x_3^α	w^α
1	1	0	0	0.01269841058
2	0	1	0	"
3	0	0	1	"
4	0.7071067812	0.7071067812	0	0.02257495612
5	0.7071067812	-0.7071067812	0	"
6	0.7071067812	0	0.7071067812	"
7	0.7071067812	0	-0.7071067812	"
8	0	0.7071067812	0.7071067812	"
9	0	0.7071067812	-0.7071067812	"
10	0.3015113354	0.3015113354	0.9045340398	0.02017333557
11	0.3015113354	0.3015113354	-0.9045340398	"
12	0.3015113353	-0.3015113354	0.9045340398	"
13	0.3015113354	-0.3015113354	-0.9045340398	"
14	0.3015113354	0.9045340398	0.3015113354	"
15	0.3015113354	0.9045340398	-0.3015113354	"
16	0.3015113354	-0.9045340398	0.3015113354	"
17	0.3015113354	-0.9045340398	-0.3015113354	"
18	0.9045340398	0.3015113354	0.3015113354	"
19	0.9045340398	0.3015113354	-0.3015113354	"
20	0.9045340398	-0.3015113354	0.3015113354	"
21	0.9045340398	-0.3015113354	-0.3015113354	"
22	0.5773502692	0.5773502692	0.5773502692	0.02109375117
23	0.5773502692	0.5773502692	-0.5773502692	"
24	0.5773502692	-0.5773502692	0.5773502692	"
25	0.5773502692	-0.5773502692	-0.5773502692	"

$\beta = 25.239401^\circ$

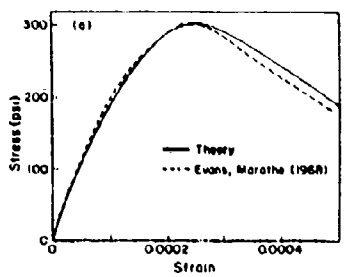

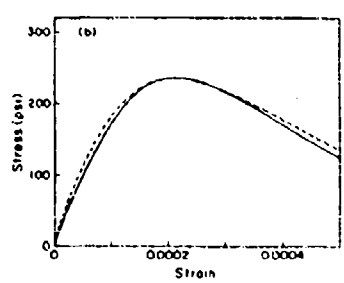

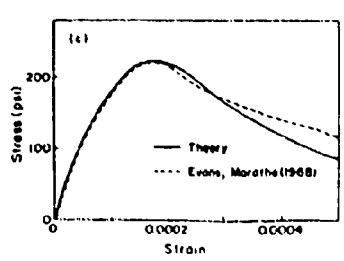

Fig. 3

Comparison with some of the Test Data of Evans and Marathe (1968)

spacing of α- directions is impossible.

Bažant and Oh [17] developed numerical integration formulas with more than 10 points, which give consistent results even in the strain-softening range. The most efficient formulas, with a nearly uniform spacing of α-directions, are obtained by certain subdivisions of the sides of an icosahedron and/or a dodecahedron [17]. Such formulas do not exhibit orthogonal symmetries. Other formulas which do were also developed [17]. Taylor series expansions on a sphere were applied and the weights w_α associated with the integration points were solved from the condition that the greatest possible number of terms of the Taylor series expansion would cancel out. The angular directions of certain integration points were further determined so as to minimize the error term of the expansion. Formulas involving 16, 21, 25, 33, 37 and 61 points were derived, with errors of 8th, 10th and 12th order [17]. Table 1 defines two of these numerical integration formulas, with 21 and 25 points, one without, and one with orthogonal symmetry. These formulas give accuracy that suffices for most pratical purposes. For crude calculations, a formula with 16 points [17] may sometimes also suffice. The directions of integration points are illustrated in Fig. 2. Also shown are stress-strain diagrams calculated with the formula for uniaxial tension in various directions with regard to the intergration points (directions a, b, c, d,...); the spread of the curves characterizes the range of error.

Numerical Algorithm

The following numerical algorithm may be used for the microplane model in each loading step.

1. Determine $\epsilon_n^{(\alpha)}$ from Eqs. 1 and 2 for all directions $\alpha = 1,...N$. In the first iteration of the loading step, use ϵ_{ij} for the end of the previous step, and in subsequent interations use the value of ϵ_{ij} determined for the mid-step in the previous iteration. In structural analysis, repeat this for all finite elements and for all integration points within each finite element.

2. For all directions $\vec{n}^{(\alpha)}$, evaluate $F'(\epsilon_n)$ for use in Eq. 7. Also check for each direction whether unloading occurs, as indicated by violation of the condition $s_n \Delta\epsilon_n \geq 0$. If violated, replace $F'(\epsilon_n)$ with the unloading stiffness (which may be approximately taken as E_n; however, a better expression exists.)

3. Evaluate D^c_{ijkm} from Eq. 7 and D_{ijkm} from Eq. 9. In structural analysis, repeat this for all elements and all integration points in each element. When solving stress-strain curves, calculate then the increments of unknown stresses and unknown strains from Eq. 9. In structural analysis, solve (by the finite element method) the increments of nodal displacements from the given load increments, and subsequently calculate the increments of ϵ_{ij} and σ_{ij} for all elements and all integration points in each element. Then advance to the next iteration of the same loading step, or advance to the next loading step.

In simulating uniaxial tensile loading of fixed direction, the unloading cirterion is not important since the only unloading occurs at moderate compressive stresses, for which a perfectly elastic unloading may be assumed.

The microplane model can be calibrated by comparison with direct tensile tests which cover the strain-softening response. Such tests, which can be carried out in a very stiff testing machine and on sufficiently small test specimens, have been performed by Evans and Marathe [20] as well as others [21-23]. Optimal values of the three parameters of the model, E_n, k, and p, have been found [19] so as to achieve the best fits of the data of Evans and Marathe. Some of these fits are shown as the solid lines in Fig. 3, and the data are shown as the dashed lines. A better test of the model would, of course, be a tensile test under rotating principal stress directions, but such tests have not yet been performed.

Note that with this theory, one has only two material parameters, E_n and k, to determine by fitting test data. Trial and error approach is sufficient for that.

Conclusion

The microplane model is capable of simulating realistic tensile stress-strain curve with strain-softening and reduction of stresses all the way to zero. Combined with the blunt crack band concept, in which the strain-softening is restricted to a region of a certain characteristic width that is a material property [1,2], this model should give a realistic representation of fracture. The model is general and does not preclude application to stress histories in which the principal stress directions rotate. These features are particularly attractive for the analysis of the response of concrete structures subjected to dynamic loads.

Acknowledgment

Partial support under Air Force Office of Scientific Research Grant No. AFOSR 83-0009 is gratefully acknowledged. Thanks are due also to Mary Hill for her careful and patient typing.

References

1. Bazant, Z. P., and Oh, B. H., "Crack Band Theory for Fracture of Concrete," Materials and Structures (RILEM, Paris), Vol. 16, 1983, in press (based on "Concrete Fracture via Stress-Strain Relations, Center for Concrete and Geomaterials, Report No. 81-10/665c, Oct. 1981, Northwestern University)

2. Bažant, Z. P., "Crack Band Model for Fracture of Geomaterials," 4th Intern. Conf. on Numerical Methods in Geomechanics, ed. by Z. Eisenstein, Univ. of Alberta, Edmonton, Vol. 3, 1982.

3. Taylor, G. I., "Plastic Strain in Metals," J. Inst. Metals, Vol. 62, 1938, pp. 307-324.

4. Batdorf, S. B., and Budiansky, B., "A Mathematical Theory of Plasticity Based on the Concept of Slip," NACA TN1871, April 1949.

5. Zienkiewicz, O. C., and Pande, G. N., "Time-Dependent Multi-laminate Model of Rocks — A Numerical Study of Deformation and Failure of Rock Masses," Int. Journal of Numerical and Analytical Method in Geomechanics, Vol. 1, pp. 219-247, 1977.

6. Pande, G. N., and Sharma, K. G., "Multi-laminate Model of Clays — A Numerical Evaluation of the Influence of Rotation of the Principal Stress Axes," Report, Dept. of Civil Engng., University College of Swansea, U.K., 1982; see also Proceedings, Symposium on "Implementation of Computer Procedures and Stress-Strain Laws in Geotechnical Engineering" Ed. By C. S. Desai and S. K. Saxena, held in Chicago, Aug. 1981, Acorn Press, Durham, N.C. 1981, pp. 575-590.

7. Pande, G. N., and Xiong, W., "An Improved Multi-laminate Model of Jointed Rock Masses," Proceedings, Intern. Symposium on Numerical Model on Geomechanics, ed. by R. Dungar, G.N. Pande, and G. A. Studer, held in Zurich, Sept. 1982, Balkema, Rotterdam, 1982, pp. 218-226.

8. Kröner, E., Zur Plastischen Verformung des Vielkristalls, Acta Metullurgica, Vol. 9, Feb. 1961, pp. 155-161.

9. Budianski, B., Wu, T. T., "Theoretical Prediction of Plastic Strains of Polycrystals," Proc., 4th U. S. Nat. Congress of Appl. Mechanics, ASME, New York 1962, pp. 175-1185.

10. Lin, T. H., Ito, M., "Theoretical Plastic Stress-Strain Relationship of a Polycrystal," Intl. J. of Engng. Science, Vol. 4, 1966, pp. 543-561.

11. Hill, R., "Continuum Micromechanics of Elastoplastic Polycrystals," J. of Mechanics and Physics of Solids, Vol. 13, 1965, pp. 89-101.

12. Lin, T. H., Ito, M., "Theoretical Plastic Distortion of a Polycrystalline Aggregate under Combined and Reversed Stresses," J. of Mechanics and Physics of Solids, Vol. 13, 1965, pp. 103-115.

13. Hill, R., "Generalized Constitutive Relations for Incremental Deformations of Metal Crystals by Multislip," J. of Mechanics and Physics of Solids, Vol. 14, 1966, pp. 95-102.

14. Rice, J. R., "On the Structure of Stress-Strain Relations for Time-Dependent Plastic Deformation of Metals," J. of Appl. Mechanics ASME, Vol. 37, Sept. 1970, pp. 728-737.

15. Bažant, Z. P., Ozaydin, K., and Krizek, R.J. "Micromechanics Model for Creep of Anisotropic Clay," J. of the Engng. Mechanics Div., ASCE, Vol. 101, 1975, pp. 57-78.

16. Calladine, C. R., "A Microstructural View of the Mechanical Properties of Saturated Clay," Geotechnique, Vol. 21, 1971, pp. 391-415.

17. Bažant, Z. P., Oh, B. H., "Efficient Numerical Integration on the Surface of a Sphere," Report No. 83-2/428e, Center for Concrete and Geomaterials, Northwestern University, Evanston, IL. 60201.

18. Albrecht, J., and Collatz, L., "Zur numerischen Auswertung mehrdimensionaler Integrale," Zeitschrift fur Angewandte Mathematik und Mechanik, Band 38, Heft 1/2, Jan/Feb., pp. 1-15.

19. Bazant, Z. P., and Oh, B. H., "Model of Weak Planes for Progressive Fracture of Concrete and Rock," Report No. 83-2/428m, Center for Concrete and Geomaterials, Northwestern University, Evanston, IL., Feb. 1983.

20. Evans, R. H., and Marathe, M. S., "Microcracking and Stress-Strain Curves for Concrete in Tension," Materials and Structures (Paris), No. 1, Jan.-Feb., 1968, pp. 61-64.

21. Heilmann, H. G., Hilsdorf, H. H., and Finsterwalder, K., "Festigkeit und Verformung von Beton unter Zugspannungen," Deutscher Ausschuss für Stahlbeton, Heft 203, W. Ernst & Sohn, West Berlin, 1969.

22. Hughes, B. P., and Chapman, G. P., "The Complete Stress-Strain Curve for Concrete in Direct Tension," Bulletin RILEM, No. 30, pp. 95-97, 1966.

23. Rusch, H., and Hilsdorf, H., "Deformation Characteristics of Concrete under Axial Tension," Vorunterschunge, Bericht Nr. 44, Munich, May 1963.